Available online at www.sciencedirect.com

jmr&t Journal of Materials Research and Technology

journal homepage: www.elsevier.com/locate/jmrt

Original Article

First-principle computations of ferromagnetic $HgCr_2Z_4$ (Z = S, Se) spinels for spintronic and energy storage system applications

Asif Mahmood [a,**], *Shahid M. Ramay* [c,*], *Waheed Al-Masry* [a], *Charles. W. Dunnill* [b], *Najib Y.A. Al-Garadi* [a]

[a] College of Engineering, Chemical Engineering Department, King Saud University Riyadh, Saudi Arabia
[b] Energy Safety Institute (ESRI), Swansea University Bay Campus, Swansea, SA1 8EN, UK
[c] Department of Physics and Astronomy, College of Science, King Saud University, Riyadh, 11451, Saudi Arabia

ARTICLE INFO

Article history:
Received 25 September 2020
Accepted 21 November 2020
Available online 27 November 2020

Keywords:
Density functional theory
Spin polarization
Ferromagnetism
Exchange splitting mechanism
Figure of merit (ZT)
Energy storage system applications

ABSTRACT

We explored electronic spin-dependent physical aspects of ferromagnetic $HgCr_2Z_4$ (Z = S, Se) spinels using density functional theory (DFT) for spintronic and energy storage applications. In calculations of structural, electronic, magnetic, and transport aspects, we used Perdew–Burke–Ernzerhof generalized gradient approximation (PBEsol GGA) plus modified Becke-Johnson (mBJ) potential. To calculate structural parameters, we optimized both spinels in the ferromagnetic phase and our predicted data of structural parameters show good comparison with existing experimental data. Also, the calculated negative formation energy confirms the structural stability of the studied spinels. Analyzing ferromagnetic nature of studied spinels based on exchange splitting energy and magnetic parameters, we used mBJ potential to calculate band structure (BS) and density of states (DOS). By exploring DOS, we found the dominant role of electrons spin has been shown by negative indirect exchange energy $\Delta_x(pd)$ values and the fulfillment of the condition $\Delta_x(d) > \Delta E_{cry}$. In addition, exchange constants ($N_0\alpha$ and $N_0\beta$) and magnetic moments were also calculated to ensure their ferromagnetism in studied spinels. Further, the exploration for the influence of electrons spin on electronic transport aspects has been done by investigating electrical and thermal conductivities, Seebeck coefficient, and power factor by using classical Boltzmann transport theory.

* Corresponding author.
** Corresponding author.
E-mail addresses: ahayat@ksu.edu.sa (A. Mahmood), schaudhry@ksu.edu.sa, smramay@yahoo.com (S.M. Ramay).
https://doi.org/10.1016/j.jmrt.2020.11.063

1. Introduction

Control of spin of electron brought a revolution in the electronic industry and introduced a new class called spintronic. For spintronic devices, we need to inject the spin of electrons in semiconducting materials. This injection of spin opens a new way in device fabrication. This is because of its low lost engineering, high efficiency, and nonvolatile storage capacity [1–3]. For this purpose, we need magnetic semiconductor and half-metallic semiconductor materials. Since most of the magnetic semiconductors are insulators and thus have advantageous. The barrier height of these insulators smoothen the spin-polarized tunneling current and thus eliminates the need for half-metallic semiconductors as an electrode material. Owing to their outstanding physical properties like giant magneto-resistance and anomalous Hall effect [4–6], ferromagnetic chalcogenide spinels like $CdCr_2X_4$ (X–S, Se) and $HgCr_2X_4$ (X = S, Se) are emerging as a potential candidate for spintronic device applications.

To exploit the potential of different compositions of spinels for various applications, we need to have a better understanding of its response towards different fields. To date, there are very limited reports on the synthesis and characterizations of ferromagnetic chalcogenide spinel $HgCr_2S_4$ especially their thin films. In the recent past, some techniques like chemical vapor deposition, non-reactive sputtering, chemical bath deposition (CBD) are used to deposit the thin films of ferromagnetic chalcogenide spinels on different substrates [7]. Among these techniques, CBD is one of the easy ways to deposit thin films because it does not require any expensive equipment for example required in chemical vapor deposition. Using CBD, one can easily deposit the thin films of typical thickness ranging from 0.02 to 1 μm thickness. This could be achieved just by dipping the substrate in dilute baths containing metals ions and a source of selenium and sulfide ions [8].

The high ferromagnetic transition temperature (106 K) of $HgCr_2Se_4$ also shows its potential for spintronic device applications [9,10]. It crystallizes in normal cubic form where Cr ions are octahedrally surrounded by Se ions giving rise to the half-filled t_{2g} states of S = 3/2. Mane et al. [11], explored optical characteristics of $CdCr_2S_4$ and $HgCr_2S_4$ thin films and they find both spinel films have n-type nature with an estimated bandgap energy Eg of 2.6 eV/2.7 eV, respectively. The crystal and magnetic interaction of $ZnCr_2S_4$ spinel is investigated by Hamedoun et al. [12] and their results show good comparison obtained between a polycrystal and a single crystal. Lattice dynamical calculations of ACr_2X_4 spinel-type chromium chalcides $CoCr_2S_4$, $ZnCr_2S_4$, ($CdCr_2S_4$), $ZnCr_2Se_4$, $CdCr_2Se_4$, and $HgCr_2Se_4$ were executed by Zwinscher et al. [13], using short-range (SRM), rigid ion (RIM) and polarizable-ion models (PIM) with structure data and calculate force constants due to the tetrahedral A-X bonds are in the order $CoCr_2S_4$ < ACr_2S_4 < ACr_2Se_4 (A = Zn, Cd, Hg). Some exceptional properties like high magneto-resistance, high hall coefficients with the red shift in optical absorption edge have further made this a ferromagnetic spinel and play a vital role for spintronic device applications [13–15]. Other theoretical literature on $HgCr_2Se_4$ represented ferromagnetism by employing the local density approximation (LDA + U) to study the exchange coupling constants [16]. Theoretically, Xu et al. [17], explored $HgCr_2Se_4$ spinel to predict the quantized anomalous Hall Effect, which was anticipated as Chern semimetal.

According to our best information, no theoretical investigation on ferromagnetism and transport aspects has been conducted on $HgCr_2Z_4$ (Z = S, Se) so far. As far as the theoretical investigation is concerned, it is very limitedly available on $HgCr_2Se_4$ in the reported literature. Therefore, in the current study, we conducted a detailed theoretical investigation on the electronic, magnetic, and transport aspects of $HgCr_2Z_4$ (Z = S, Se). For this, DFT based technique revised by modified Becke and Johnson (as implemented in Wein2K code) has been applied in our study [18]. This technique in turn produced the exact electronic structures of the spinels with accurate bandgaps. For the judgment of the consistency in transport aspects, the computed electronic structures were integrated with BoltzTraP code [19]. The revealed structural stability in the ferromagnetic phase and computed transport aspects of studied spinels demonstrated them useful in the applications related to spintronic and energy storage devices.

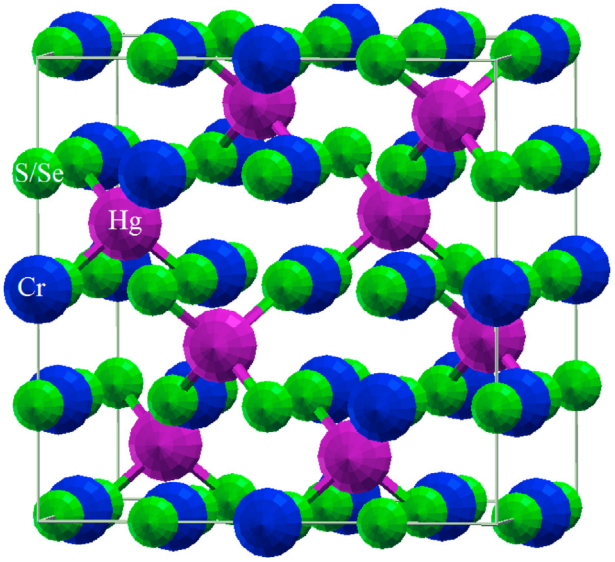

Fig. 1 – Crystal structure of spinels $HgCr_2Z_4$ (Z = S, Se). Pink, blue and green spheres represent Hg, Cr, and S/Se atoms, respectively. (For interpretation of the references to color in this figure legend, the reader is referred to the Web version of this article.)

2. Method of calculation

In this paper, we employed a spin-polarized DFT computational method to investigate the electronic, magnetic, and transport aspects of $HgCr_2Z_4$ (Z = S, Se), where similar systems are already theoretically reported [20–23]. The method used for all studied calculations is full-potential linearized augmented plane wave plus local orbital (FP-LAPW + lo), which is implemented in Wien2k software [24]. PBEsol generalized gradient approximation of Perdew et al. [18], was adopted for the computation of the ground-state energies and

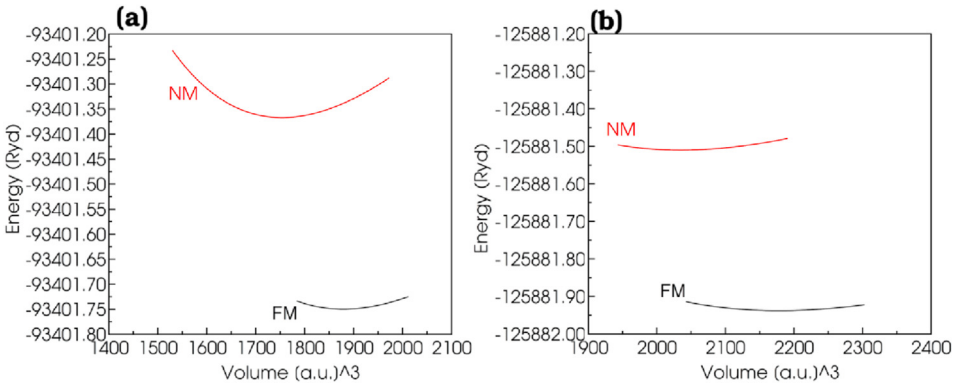

Fig. 2 – The energy versus volume plots of (a) $HgCr_2S_4$ and (b) $HgCr_2Se_4$ spinels in FM and NM phases.

structural parameters, in particular with exchange-correlation functionals. The structures were continued to be optimized until all the forces on each atom fall to zero. Further, the Tran–Blaha-modified Becke–Johnson (TB-mBJ) [25] exchange potential has also been brought into use for the investigation of the electrons spin-dependent ferromagnetic and transport aspects. Because, literatures show that TB-mBJ potential is useful as exchange-correlation functionals in predicting the electronic band structure [26,27]. The muffin-tin radius (R_{MT}) and the maximum value of the wave vector (K_{max}) are multiplied as $R_{MT} \times K_{max} = 8$ in reciprocal lattice for the convergence of the energy. So for better convergence, we take $R_{MT} \times K_{max} = 8$ for all calculations.

In addition, we set muffin-tin radii as 2.37 a.u. for Cu, 2.5 a.u. for Cr, 1.85 a.u. for S, and 2.1 a.u for Se. The default value (-6Ry) of cut off energy was employed. Furthermore, the angular momentum vector (l_{max}) and Gaussian factor (G_{max}) have been kept at 10 Ry and 18 Ry respectively. The primary and essential point of methodology is the selections of k-points, which are chosen by selecting the number of k-points pairs for the best conversion of energy. For best energy convergence, 1000 k-points are selected because, after these k points, energy optimizations become constant. For transport aspects, the semi-classical Boltzmann transport theory has been employed to compute the $HgCr_2Z_4$ (Z = S, Se) [28,29]. Moreover, for the transport aspects, all the calculations related to the electronic structure of the spinels have been used within the BotlzTraP code [19]. For all the BoltzTrap calculations, a larger value of k points is used in this study, and electrical (σ) and thermal (κ) conductivities, Seebeck coefficient (S), and figure of merit (ZT) have been investigated against the temperature range 200 K–600 K.

Table 1 – The calculated lattice constant a_0 (Å), bulk modulus B_0 (GPa) ground state energy difference ($\Delta E = E_{NM} - E_{FM}$), enthalpy of formation ΔH (eV) for $HgCr_2Z_4$ (Z = S, Se).

Spinels	a_0 (Å)	B_0 (GPa)	ΔE (eV)	ΔH (eV)
$HgCr_2S_4$	10.37	90.15	5.21	−0.98
Exp.	10.24[a]			
$HgCr_2Se_4$	10.89	72.83	6.64	−0.84
Exp.	10.75[a]			

[a] Ref [34].

3. Results and discussion

3.1. Structural and electronic properties

The cubic spinels $HgCr_2Z_4$ (Z = S, Se) that possess space group Fd-3m#227 (see Fig. 1) and are of ordered crystalline structures have been converged with reference of energy for the minimization of their ground state energies in non-magnetic (NM) and ferromagnetic (FM) states. The plots of the energy (Ry) versus volume (a.u.) in terms of NM and FM states have been shown in Fig. 2 (a, b). It is clear from the comparative analysis that FM state is responsible for higher energy release than that of NM State. This confirms the more stability of FM than that of NM states. From Refs. [30,31], we can see that the studied compounds are experimentally found to be ferromagnetic. In order to justify that our calculations agree with the experimental results, we have only considered nonmagnetic and ferromagnetic configurations of the spins. As evident from our calculations, DFT also predicts $HgCr_2Z_4$ to be stable ferromagnetic compounds. In addition, the enthalpy of formation (ΔH_f) is computed to find out the thermodynamic stability of the said cubic spinels. ΔH_f can be found by using the following expression [32]:

$$\Delta H_f = E_{Total}(Hg_lCr_mZ_n) - lE_{Hg} - mE_{Cr} - nE_Z \quad (1)$$

here, $E_{Total}(Hg_lCr_mZ_n)$ is the total calculated ground state energy of studied spinels, while E_{Hg} E_{Cr} E_Z, represents their individual atoms energies. The letters l, m, and n represent the number of atoms of Hg, Cr, and S/Se per their unit cell volume, correspondingly. Referred to Table 1, our calculated values of ΔH_f represent negative values. It means that studied spinels with negative values thermodynamically stable. The decrease in the stability happens when S is replaced with Se.

To find the ground states lattice parameters such as the lattice constant (a_o) and bulk modulus B_0, we done volume optimization in FM phase. From the minimum volume of the unit cell, we calculate a_o and B_0 using Murnaghan's equation of state [33] with PBEsol-GGA. The results of both parameters are tabulated and noted that the calculated value of a_o for both spinels are closely related to experimental values [34]. The

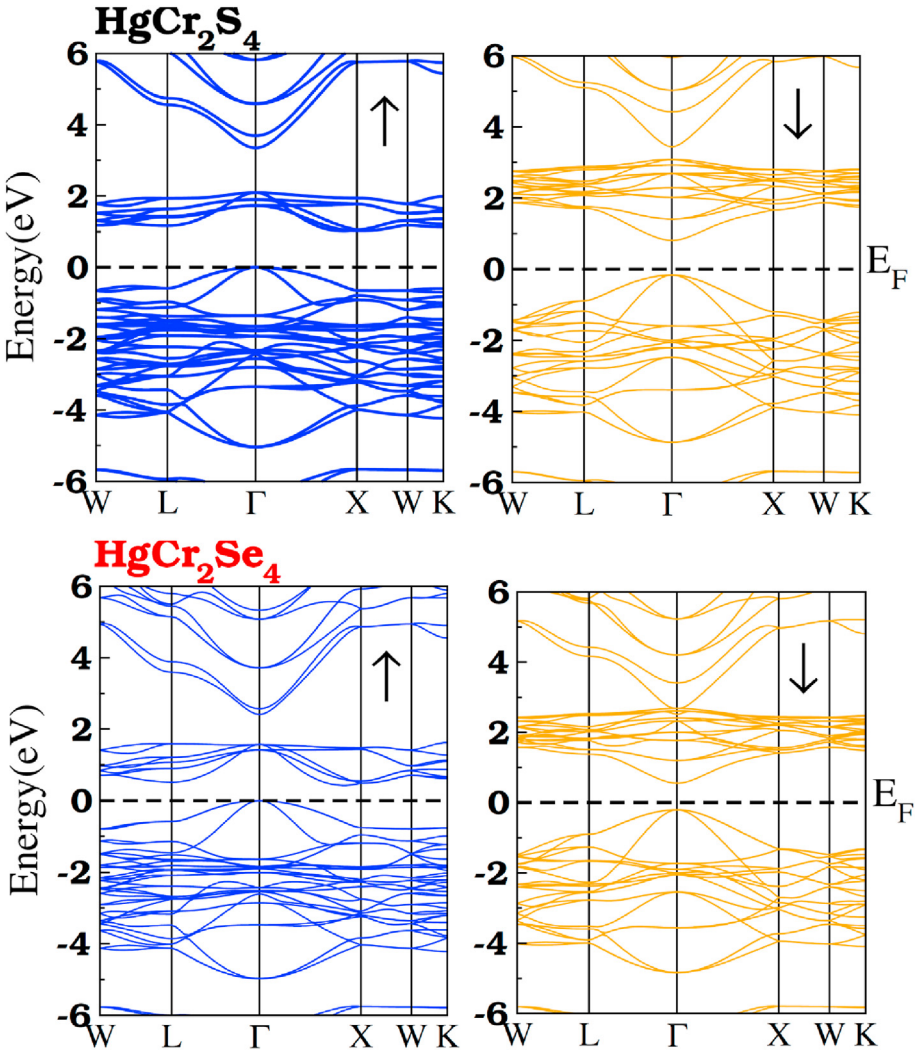

Fig. 3 – Spin dependent band structures plot for $HgCr_2S_4$ and $HgCr_2Se_4$ for majority spin (↑) and minority spin (↓) channels.

bulk modulus decreases whereas there is an increase in lattice constant from $HgCr_2S_4$ to $HgCr_2Se_4$. This happens because interatomic distance starts increasing when the anion size increases.

Further, the electronic behavior of any substance is very important to be computed because it has a direct effect on other physical features such as electronic transport and magnetic aspects. However, for its detailed description, an in-depth study of band structure (BS) is considered extremely significant. For the accurate prediction of BS, we employed TB-mBJ potential for $HgCr_2Z_4$ (Z = S, Se). Therefore, the detailed description of the calculated BS has been shown in Fig. 3. The location of conduction band minima is at X-symmetry direction whereas the location of valence band maxima is at Γ-symmetry direction with Fermi level at valence band in up spin (↑) channel. In the up spin (↑) channel, the indirect bandgap with the semiconducting behavior of the spinels is clear. On the other hand, the same location at Γ-symmetry direction for both conduction band minima and valence band maxima has been found to observe in down spin (↓) channel, with Fermi level inside them. This produces an insulating bandgap with the exchange of mechanism. The combination of down spin (↓) channel along with insulating and up spin (↑) channel with semiconducting properties makes the ferromagnetic semiconductors. The calculated values of up spin (↑) bandgap for studied spinels are listed in Table 1 and we found our calculated values of bandgap indicate that these spinels can function invisible of the electromagnetic spectrum.

The total density of states (TDOS) shows also a similar type of behavior (see Figs. 4 and 5). The TDOS along with partial density of states (PDOS) Hg, Cr, and S/Se illustrates the ferromagnetism and exchange mechanism (see Figs. 4 and 5). In up spin channel, there is hybridization of individual Hg-2s/2p states and Cr-3d-states in the region between −2.8 eV and 2.0 eV and −4.0 eV to Fermi level with S/Se-2p states. On the other hands, it is −1.4 eV to −3.0 eV Cr-3d states, Hg-2s/2p and S/Se-2p states respectively in down spin channel. Further, in the conduction band, the hybridization of Cr-3d states, Hg-2s/2p states, and S/Se-2p states is from 1.0 eV to 2.2 eV for spin-down channel and from 1.4 eV to 3.2 eV for up spin channel. However, in the down spin channel, the splitting of states and interaction inside the valence band are considered accountable for the exchange mechanism to induce ferromagnetic semiconducting nature in the spinels.

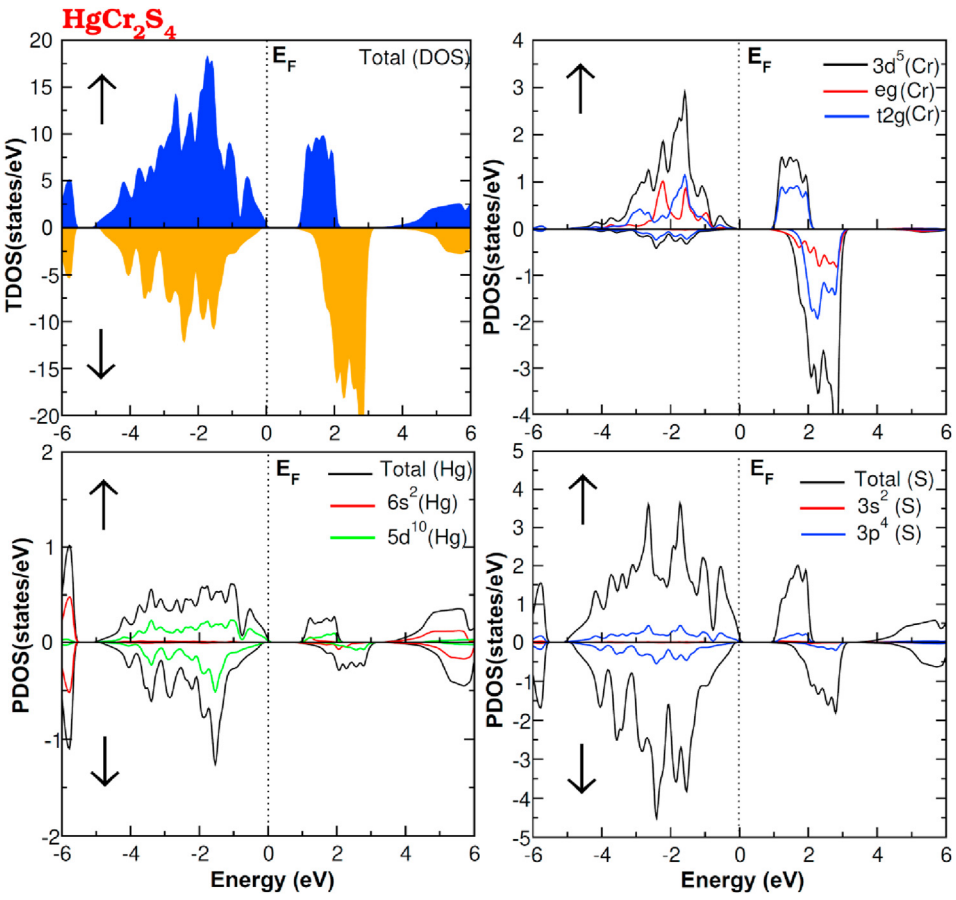

Fig. 4 – The TDOS of $HgCr_2S_4$ spinel and their PDOS of Cr, Hg and S atoms for up (↑) and down spin (↓) channels.

3.2. *Magnetic properties*

The partial and total magnetic moment (μ_B) of the spinels has been shown in Table 2 to show the absence of the clustering of transition metal (Cr) and to explain the exchange energies as a source of ferromagnetism. The exchange interaction in S/Se-*p* states Cr-3*d* states becomes clear from the shifting of magnetic moment to nonmagnetic sites and from the decreasing of magnetic moment of Cr atom. Moreover, various exchanges may also be involved in the structures causing the shifting magnetic moments towards interstitial regions.

The exchange energies and crystal fields are produced by the hybridization of the individual states in the structures of the compounds in hand. The octahedron of S/Se atoms occupies the Cr site with +3 valencies, whereas the tetrahedral setting of S/Se atoms occupies the Hg site of valency +2. A coulomb repulsive effect having 3 d electrons of Cr atoms is thus generated by the octahedral positions of S/Se, which proves to be more powerful near the octahedron and becomes comparatively weaker away from it. The 3 d states of Cr are split into triplet (linear, t_{2g}) and doublet states (nonlinear, e_g) by the octahedral environment of S/Se atoms because of which the elongation happens in octahedron while raising the energy of e_g states as compared with the t_{2g} states [35–37]. The calculated energy of the crystal field such as $\Delta E_{cry} = t_{2g} - e_g$ of studied spinels are expressed in Table 3. When we calculated the crystal field energy and exchange splitting of 3 d states of Cr with the help of relation;$(\Delta_x(d) = \Delta_d^{\downarrow} - \Delta_d^{\uparrow})$ we found that the crystal field energy holds a lower value as compared with the exchange energy. Resultantly, the greater value of exchange energy is due to the dominance of ferromagnetism.

S/Se-*p* states and Cr-3*d*-states induce one another kind of energy that was measured by indirect exchange energy $\Delta_x(pd)$. Here, the negative indirect exchange energy $\Delta_x(pd)$ favors the ferromagnetism by demanding lower energy. The exchange energy $\Delta_x(d)$ and indirect exchange energy $\Delta_x(pd)$ increase from $HgCr_2S_4$ to $HgCr_2Se_4$ as shown in Table 3, whereas Δ_{CF} decreases proving $HgCr_2Se_4$ more favorable for ferromagnetism as compared with $HgCr_2S_4$. Through the relations such as $N_0\beta = \Delta E_V / x\langle S\rangle$, and $N_0\alpha = \Delta E_C / x\langle S\rangle$ [38,39], the exchange constants have been computed, which further elucidate the ferromagnetism. In the relations, $(\Delta E_C = E_C^{\downarrow} - E_C^{\uparrow})$ and $(\Delta E_V = E_V^{\downarrow} - E_V^{\uparrow})$ are the energies at conduction and valence bands, where $\langle S\rangle$ is the average magnetic moment of Cr atom and X is the concentration of magnetic ions. The negative value of $(N_0\beta)$ and $(N_0\alpha)$ as shown in Table 3 are considered the typical trends of ferromagnetic semiconductors. The magnetic impurity is revealed by the negative value of $(N_0\beta)$

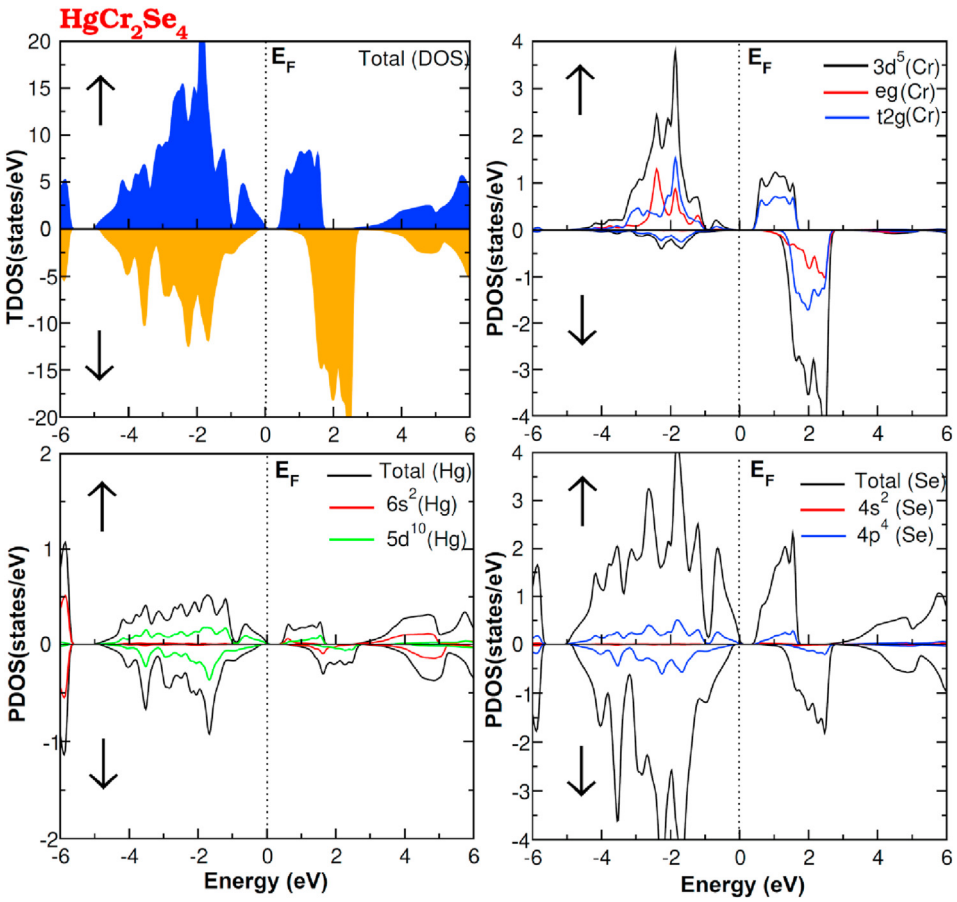

Fig. 5 – The TDOS of $HgCr_2Se_4$ spinel and their PDOS of Cr, Hg and Se atoms for up (↑) and down spin (↓) channels.

through energy gaps in down spin channel, due to the energy decreases to favor the Zenger's exchange model [40,41].

3.3. *Electronic transport behavior*

It is very important to know about the electronic transport behavior of spin orientated compounds for device fabrication [42,43]. The ability of devices to convert the wasted heat into beneficial electrical energy is illustrated by the transport parameters. It is, therefore, electronic transport behavior of $HgCr_2Z_4$ (Z = S, Se) is brought into detailed discussion in terms of figure of merit (ZT), power factor ($\sigma S^2/\tau$), Seebeck coefficient (S), thermal conductivity (κ/τ), and most importantly, electrical conductivity (σ/τ), in temperature ranges from 200 to 600 K (see Figs. 6(a-d) and 7.

The movement of free carriers shows the electrical conductivity (σ/τ). When the temperature is increased, the σ/τ of ferromagnetic spinels starts increasing because sufficient energy is provided to the carriers by the temperature that allows the movement of the carriers towards the conducting channel from the valence one. The σ/τincreases gradually up to 600 K for both spines under observation. The increasing rate of σ/τ of $HgCr_2S_4$ falls slow as compared with $HgCr_2Se_4$ (see Fig. 6a). So, $HgCr_2S_4$ carries the highest σ/τup to 600 K, where the rest of the studied spinel may fall victim to thermal agitation. However, the carriers and the lattice vibration produce heat in ferromagnetic spinels for κ/τ as phonon wave is produced by lattice vibration. Due to the limitations of classical transport theory-based BoltzTraP code [19], we have managed to study only the electronic part of κ_e/τ.

To understand the thermal conductivity of both spinels, the Fourier law ($q = -\kappa\, dT/dx$) [44,45] proves to be very helpful for us where efflux of heat is represented by q, temperature gradient is represented by dT/dx, and coefficient of κ_e/τ is represented by κ_e. Up to 400 K, there is a gradual increase in the κ/τ of the studied spinels after which it becomes comparatively fast as the carriers become more energetic to

Table 2 – The total and the local magnetic moments (in Bohr magneton) calculated for $HgCr_2Z_4$ (Z = S, Se).

Spinels	Total (μ_B)	Int.(μ_B)	Hg (μ_B)	Cr (μ_B)	($Z\mu_B$)
$HgCr_2S_4$	12.0009	0.34	0.003	3.007	−0.047
$HgCr_2Se_4$	12.0006	0.31	0.008	3.085	−0.079

Table 3 – The calculated values spin down gap ($\uparrow E_g$ (eV)), crystal field energy ($\Delta E_{crystal}$), direct exchange $\Delta_x(d)$ and indirect exchange $\Delta_x(pd)$ and the exchange constants ($N_o\alpha$ and $N_o\beta$) for $HgCr_2Z_4$ (Z = S, Se).

Spinels	$\uparrow E_g$	($\Delta E_{crystal}$)	$\Delta_x(d)$	$\Delta_x(pd)$	$N_o\alpha$	$N_o\beta$
$HgCr_2S_4$	0.90	3.80	4.10	−0.15	−0.20	−0.08
$HgCr_2Se_4$	0.35	3.38	3.90	−0.11	−0.39	−0.06

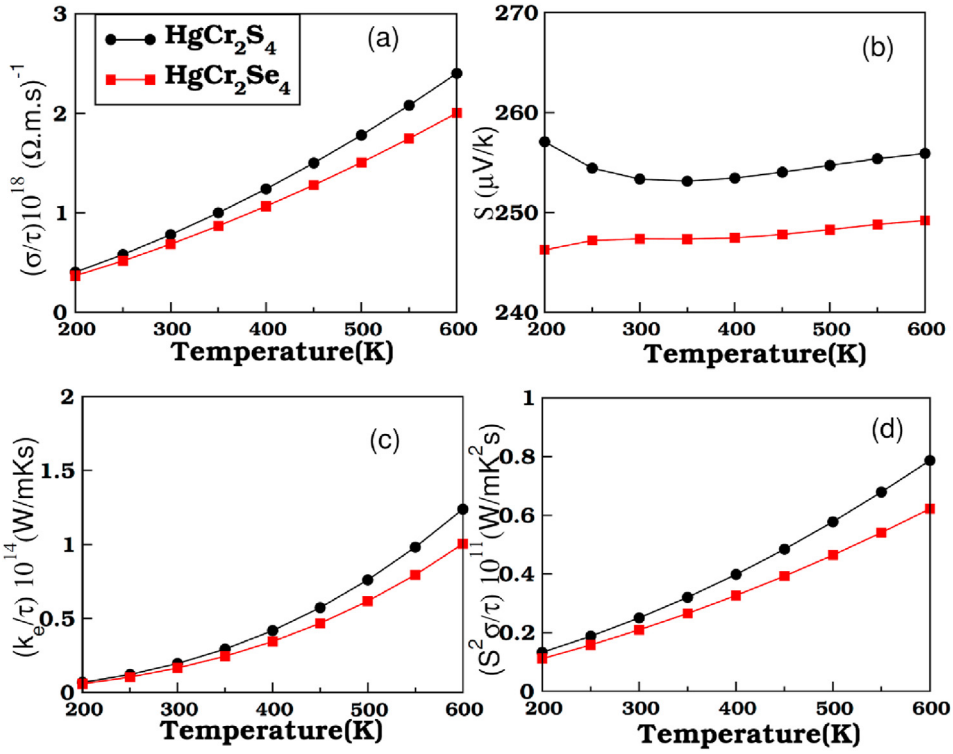

Fig. 6 – The computed (a) electrical conductivity (σ/τ), (b) Seebeck coefficients, (c) electronic thermal conductivity (k_e/τ) and (d) power factors ($S^2\sigma/\tau$) plot versus temperature of $HgCr_2S_4$ and $HgCr_2Se_4$ spinels.

flow in more heat. However, $HgCr_2Se_4$ has the least κ/τ at 600 K, whereas at the same temperature range, $HgCr_2S_4$ achieves the highest level of it (see Fig. 6c). There must be a very low ration of κ/τ to σ/τ (Weidman-Franz law (LT = κ/σ)) against temperature to be the best thermoelectric materials. Its value is of the order of 10^{-6} indicating the compounds useful in thermoelectric applications.

The calculation of the temperature gradient of potential is done as the See back coefficient (S) between two dissimilar metals. Fig.6b shows the computed value of S of the materials. It has a small value for $HgCr_2Se_4$ and a large one for $HgCr_2S_4$ at 200 K. Further, the Seebeck coefficient has convergence at 250 K whereas it has divergence up to 600 K for both spinels under experiment. $HgCr_2S_4$ secured maximum value whereas $HgCr_2Se_4$ attained minimum value from all the materials. In addition, the p-type behavior of the studied spinels becomes clear from the positive value of See back coefficient. The thermoelectric efficiency is measured by the power factor ($S^2\sigma/\tau$). It does not include thermal conductivity because of which its resulted values are overestimated, but at the same time, the trends have accuracy. There was an increase in the value of power factor up to 600 K for both spinels. For both spinels $HgCr_2Se_4$ and $HgCr_2S_4$, its value becomes constant on the same temperature range. On the other hand, its value continued to increase linearly up to 600 K for $HgCr_2S_4$, (see Fig. 6d). The small Seebeck coefficient causes an increase in the power factor at higher temperatures [46,47]. Lastly, we also investigate the figure of merit (ZT) using the known values of σ, S, and *ke* and found linear variation with temperature range (200 K–600 K). From Fig. 7, a ZT value with temperature varies directly and recorded maximum values at 600 K for both spinels $HgCr_2S_4$ and $HgCr_2Se_4$.

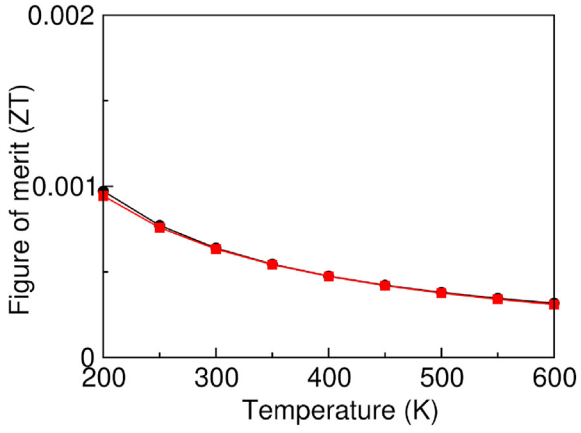

Fig. 7 – The computed figure of merit (ZT) plot versus temperature of $HgCr_2S_4$ and $HgCr_2Se_4$ spinels.

4. Conclusions

In the current study, BoltzTraP code and Wien2k code have been brought into use for the electronic transport and ferromagnetism aspects of $HgCr_2Z_4$ (Z = S, Se). More energy was released in FM than that of NM State during the optimizing process where the ferromagnetism has further been assured by negative values of ΔH_f. The ground state parameters such as B_0 decrease whereas there is an increase in a_0 from $HgCr_2S_4$

to $HgCr_2Se_4$ in FM phase and noted that our calculated values of a_0 good comparable to experimental value. The DOS and the electronic BS of the studied spines prove them to be ferromagnetic semiconductors. From DOS, we calculate the exchange interactions and found strong hybridization that ensures the ferromagnetism tempted by electrons spin. Our predicted results of exchange parameters indicate that comparatively greater values of $\Delta(d)$ are favorable for the ferromagnetism than (Δ_{CF}). In addition, the exchange constant $(N_0\beta)$ and the negative value of-exchange energy are the cause of reduction in energy in the down spin channel. Another evidence for p-d hybridization/exchange interaction is the decrease of μ_B at Cr site and increase of μ_B on other sites. The κ/σ ratio and power factor prove that more thermoelectric efficiency is possessed by $HgCr_2S_4$ than $HgCr_2Se_4$.

Declaration of Competing Interest

There is no conflict of interest.

Acknowledgment

The authors extend their appreciation to the Deputyship of Research & Innovation, "Ministry of Education" in Saudi Arabia for funding this research work through project No. IFKSURG-311.

REFERENCES

[1] Biswas P, Mamatha S, Naskar S, Rao YS, Johnson R, Padmanabham G. J Alloys Compd 2019;770:419–23.
[2] Canepa P, Bo SH, Gautam GS, Key B, Richards WD, Shi T, et al. Nat Commun 2017;24:1–8.
[3] Pang C, Srivastava A, Lockart MM, Mewes T, Bowman MK, Bao N, et al. ACS Appl Electron Mater 2019:1424–32.
[4] Solin NI, Chebotaev NM. Phys Solid State 1997;39:754.
[5] Solin NI, Ustinov VV, Naumov SV. Phys Solid State 2008;50:901.
[6] Mane RS, Lokhande CD. Mater Chem Phys 2000;65:1.
[7] Deshmukh LP, Holikatti SG, Rane BP, Belle MI, Hankare PP. Bull Electrochem 1993;9:237.
[8] Mane RS, Todkar VV, Lokhande CD, Kalea SS, Han Sung-Hwan. Vacuum 2006;80:962–6.
[9] Lehmann W, Emmenegger FP. Solid State Commun 1969;79:65.
[10] Solin NI, Ustinov VV, Naumov SV. Phys SolidState 2008;50:901.
[11] Mane RS, Sankapal BR, Gadave KM, Lokhande CD. Mater Res Bull 1999;34:2035.
[12] Hamedoun M, Hourmatallah A, Sayouri S, Chatwiti A. J Phys Condens Matter 1995;7:5359.
[13] Zwinscher J, Lutz HD. J Solid State Chem 1995;118:43–52.
[14] Solin NI, Chebotaev NM. Phys Solid State 2008;39:754.
[15] Arai T, Wakaki M, Onari S, Kubdo K, Satoh T, Tsushima T. J Phys Soc Jpn 1973;34:68.
[16] Yaresko AN. Phys Rev B 2008;77:115106.
[17] Xu G, Weng HM, Wang ZJ, Dai X, Fang Z. Rev Lett 2011;107:186806.
[18] Tran F, Blaha P. Phys Rev Lett 2009;102:22640.
[19] Madsen GK, Singh DJ. Comput Phys Commun 2006;175:67.
[20] Yang Juntao, Zhou Yong, Dedkov Yuriy, Elena Voloshina. Adv Theory Simul 2020;3:2000228.
[21] Yanga Juntao, Zhou Yong, Guo Qilin, Dedkov Yuriy, Elena Voloshina. RSC Adv 2020;10:851.
[22] Li Xingxing, Wu Xiaojun, Yang Jinlong. J Am Chem Soc 2014;136(31):11065–9.
[23] Zhang X, Zhao X, WuYu D, Zhen Zhou J. Adv Sci 2016;3:1600062.
[24] Blaha P, Schwarz K, H Madsen GK, Kvasnicka D, Luitz J. WIEN2k; an augmented planewave plus local orbital program for calculating crystal properties. Austria: Vienna University ofTechnology; 2001.
[25] Perdew P, Ruzsinszky A, Csonka GI, Vydrov OA, Scuseria GE, Constantin LA, et al. Phys Rev Lett 2008;100:136406.
[26] Noor NA, Ali S, Murtaza G, Sajjad M, Alay-e-Abbas SM, Shaukat A. Comput Mater Sci 2014;93:151–9.
[27] Noor NA, Rashid M, Alay-e-Abbas SM, Raza M, Mahmood A, Ramay SM. Mater Sci Semicond Process 2016;49:40–7.
[28] Nag BR. Electron transport in compound semiconductors, vol. 11. Springer Science & Business Media; 2012.
[29] Scheidemantel T, Ambrosch-Draxl C, Thonhauser T, Badding J, Sofo J. Phys Rev B 2003;68:125210.
[30] Lehmann HW, Emmenegger FP. Solid State Commun 1969;7:965–8.
[31] Hastings JM, Corliss LM. J Phys Chem Solid 1968;29:9–14.
[32] Mahmood Q, Noor NA, Jadan M, Addasi Jihad S, Mahmood Asif, Ramay ShahidM. J Solid State Chem 2020;285:121261.
[33] Murnaghan FD. Proc Natl Acad Sci USA 1944;30:244–7.
[34] Konopka D, Kozlowska I, Chełkowski A. Phys Lett A 1973;44:289–90.
[35] Walsh A, Wai SH, Yan Y, Al-Jassim MM, Turner JA. Phys Rev B 2007;76:165119.
[36] Choi HC, Shim JH, Min BI. Phys Rev B 2006;74:172103.
[37] Kumar A, Fennie CJ, Rabe KM. Phys Rev B 2012;86:184429.
[38] Hassan M, Arshad I, Mahmood Q, Semicond. Sci Technol 2017;32:115002.
[39] Noor NA, Ali S, Tahir W, Shaukat A, Reshak AH. J Alloys Compnd 2011;509(32):8137–43.
[40] Mahmood Q, Rashid,Qurat-ul-Ain M, Noor NA, GulBaharAshiq M, Ramay ShahidM, Mahmood A. J Mol Graph Model 2019;88:168–73.
[41] Kant C, Deisenhofer J, Tsurkan V, Loidl A. J Phys: Conf Seri 2010;200:032032.
[42] Ali S, Rashid M, Hassan M, Noor NA, Mahmood Q, Laref A, et al. Phys B Condens Matter 2018;537:329–35.
[43] Majid Farzana, Hassan MTauqeerM, Arshad I, Mahmood Q. Semicond Sci Technol 2017;32:115002.
[44] Nasir EmanAlgrafy, Sajjad Muhammad, Noor NA, Mahmood Asif, Ramay ShahidM. J Mater Res Technol 2020;9:6135–42.
[45] Noor NA, Anwar U, Mahmood A. Chem Phys Lett 2020;739:137031.
[46] Bilal, Saifullah M, Shafiq M, Khan B, Aliabad HAR, Asadabadi SJ, Ahmed R, et al. Phys Lett A 2015;379:206–10.
[47] Liu C, Morelli DT. J Electron Mater 2011;40(5).